Calculation of Eigenmodes in a Nonperiodic Corrugated Waveguide

Ioannis G. Tigelis, *Member, IEEE*, Marco Pedrozzi, P. G. Cottis, and John L. Vomvoridis

***Abstract*—A theoretical technique for determining the dispersion relation, the electromagnetic field components, and the quality factor of a dielectric-loaded nonperiodic corrugated waveguide is presented for the case of azimuthally symmetric TM waves. The Floquet theorem is used to express the field distribution in the vacuum region, while an eigenfunction expansion is employed in each dielectric region, with the appropriate boundary conditions applied at the interfaces, leading to an infinite system of equations. This system is solved numerically by truncation, while the convergence of the solution is examined with the number of spatial harmonics. Based on this formulation, a numerical code, called *FISHBONE-TM*, is developed and its results are compared with those obtained with an established code (*CASCADE*) based on the scattering-matrix method.**

***Index Terms*— Bloch harmonics, corrugated waveguide, gyrotron-beam tunnel.**

I. Introduction

THE GYROTRON is an inherently fastwave electron-beam device which approximately operates at the gyrofrequency of the electrons (with a small Doppler shift) in an axial magnetostatic field. For high-power performance, the properties of the electron beam (in particular, the ratio $p_\perp/p_\parallel$ of transverse to longitudinal momentum and the current density carried by the beam) need to be adjusted from the values produced by the electron gun to those required in the gyrotron cavity. This is accomplished in the beam tunnel (the region between the electron gun and the gyrotron cavity), by increasing the axial magnetostatic field. To prevent the gyrotron interaction from occurring prematurely in the latter part of the beam tunnel (where the ratio $p_\perp/p_\parallel$ reaches values high enough) rather than in the gyrotron cavity [1]–[3], the interior walls of the beam tunnel are lined with a lossy material, interlaced with metal rings to collect any stray electrons and prevent them from depositing on the dielectric. For good behavior of the lossy material in the presence of the high-quality vacuum of the tube, the available choices limit the loss tangent generally to about 0.1, although values as high as 0.33 have also been reported [1].

In the structure just described, replacing the dielectric rings by vacuum indentations with electrically equal dimensions and distributing the losses on the wall (rather than in the dielectric volume), the electrodynamically identical corrugated waveguide is produced. Such structures are widely used to distribute the interaction of the electrons with the electromagnetic waves along the entire structure of a traveling-wave tube (TWT) and to avoid reflections and oscillations in the extraction sections [4] or as mode converters [5]. Of course, in spite of their equivalence, these two applications of corrugated waveguides are serving radically different purposes: to generate a wave in the TWT and to suppress any wave growth in the gyrotron-beam tunnel.

In either of those realizations of a corrugated waveguide (i.e., in the gyrotron-beam tunnel and in the TWT), the structure is typically periodic with the period consisting of one metal ring and one dielectric ring (or one indentation). Periodic-guiding structures are employed in microstrip-array slow-wave structure (SWS) [6], in gyro traveling-wave amplifier (TWA) operations [7], or in TWT's and oscillators [8], [9]. Their dispersive characteristics have been analyzed either in the frequency domain [7]–[10] or in the time domain [11]. The field analysis of such a structure is straightforward [12]–[14]: The Floquet theorem is invoked to represent the propagating wave in the inner region as an infinite sum of Bloch components, while the fields in the dielectric rings (or the indentations) are represented by an infinite sum of the corresponding standing eigenwaves. Then, the appropriate boundary conditions at the interface of the inner region with the dielectric rings (or indentations) and with the conducting walls are imposed. Application of the orthogonal properties of the eigenfunctions yields the dispersion relation $\omega(k)$ in the form of a determinantal equation of infinite size, which is truncated to finite size for numerical calculations.

It is apparent that deviations from periodicity would modify both the frequency response $\omega(k)$ and the field distribution along the corrugated waveguide. Whether and when such modifications represent an improvement (i.e., a stronger interaction for the TWT) or a weaker interaction easily absorbed by the lossy dielectric in the gyrotron-beam tunnel remains to be studied. For such a study, the field analysis of any given geometry is called upon to produce: 1) the frequency spectrum $\omega(k)$, in order to identify possible resonances of the guided wave with the electron beam (e.g., by equating $\omega(k) = kv_\parallel$ for the axial interaction involved in the TWT) and 2) the relative

Manuscript received February 1, 1996; revised October 18, 1996. This work was supported in part by the Fusion Programme of the European Commission (EC) under contracts ERB 5000 CT 920028 and ERB 5000 CT 940020. The work of I. G. Tigelis and J. I. Vomvoridis was conducted in part at CRPP, Lausanne, Switzerland, under a mobility contract supported by the EC.

I. G. Tigelis is with the University of Athens (UoA), Physics Department, Applied Physics Division, Panepistimiopolis, Athens, Greece.

M. Pedrozzi is with the Ecole Polytechnique Federale de Lausanne (EPFL), Centre de Researches en Physique des Plasmas (CRPP), PPB Ecublens, Lausanne, Switzerland.

P. G. Cottis and J. L. Vomvoridis are with the National Technical University of Athens (NTUA), Department of Electrical and Computer Engineering, Athens, Greece.

Publisher Item Identifier S 0018-9480(97)00828-4.

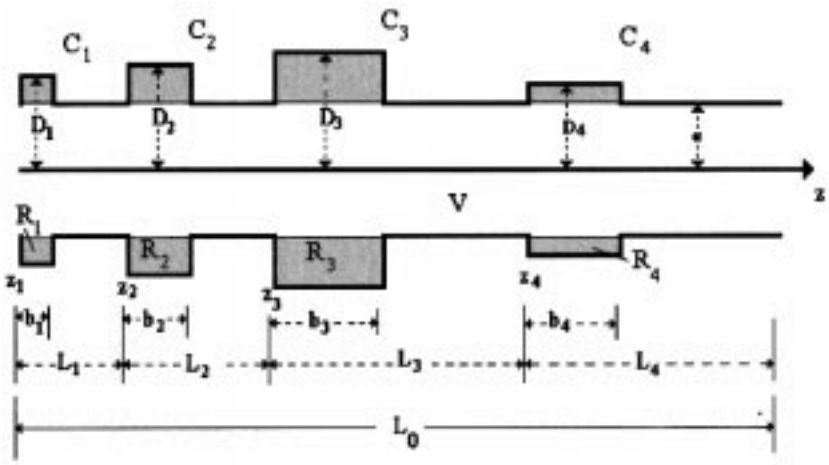

Fig. 1. The geometry of a cylindrical nonperiodic corrugated waveguide.

amplitude and spatial distribution of the resonant component of the wave to calculate its coupling to the electron beam.

The geometry of a cylindrical nonperiodic corrugated waveguide is shown in Fig. 1, where the cylindrical coordinates (ρ, φ, z) are employed. Over a total length L_0, the inner vacuum region extends radially to the radius $\rho = \alpha$. Beyond this radius are located the dielectric rings (from $z = z_i$ to $z = z_i + b_i$) with outer radius D_i, thickness $b_i (< L_i)$, and complex permittivity ε_i. The conductor extends both beyond (for $\rho > D_i$) and between (for $\rho > \alpha$, when $z_i + b_i < z < z_i + L_i = z_{i+1}$) the dielectric rings. Lack of periodicity means that one or more of the quantities D_i, ε_i, L_i, and b_i are distributed unevenly.

An analytical approach to calculate the wave field structure in a geometry like that of Fig. 1 (i.e., with abrupt changes at the positions $z_i, z_i + b_i$, etc.) involves three steps: First, the fields in each segment are expanded in transverse radial and azimuthal eigenfunctions to obtain their axial dependence for any given frequency ω. Second, the appropriate boundary conditions are imposed at each interface (including the endpoints $z = 0$ and $z = L_0$) to interrelate the coefficients of each eigenfunction expansion. Third, the dispersion relation $k(\omega)$ is obtained by Fourier-transforming the axial dependence of the fields. For a total number of P dielectric rings, this approach amounts to dividing the corrugated waveguide into $(2P + 1)$ regions and applying the boundary conditions at an equal number of $(2P + 1)$ interfaces. This approach has been implemented in the *CASCADE* code [15], [16].

An alternate approach, proposed and implemented in this paper, again involves three steps: First, the fields are expanded in azimuthal and axial eigenfunctions (with the input/output conditions at $z = 0$ and $z = L_0$ defining a Sturm–Liouville problem for the fields in the vacuum inner region), leading to the corresponding radial dependence for any given frequency. Second, the appropriate boundary conditions are imposed to interrelate the coefficients of each eigenfunction expansion. Third, the summation over the eigenfunctions is performed to obtain, if needed, the axial distribution of the total field. In this approach, the system is divided in $(P+1)$ regions and an equal number of boundary conditions is involved (at $\rho = \alpha$, one outwards and P inwards). For a periodic system it suffices to take the special case $P = 1$.

Two distinct advantages can be expected from the approach developed in the present paper: First, a smaller number of numerical operations is involved. (However, not in the ratio $(P + 1)/(2P + 1) \cong 0.5$, since the long vacuum region is expected to require more terms for convergence.) Second, if the information obtained is to be used eventually to study the interaction of the guided waves with an electron beam, then the dispersion relation $\omega(k)$ and the relative amplitudes of the various axial modes are the only information actually needed. In our approach, this information is obtained in the second step, and the third step is (in this context) completely redundant.

On the other hand, keeping a constant inner-radius α is a built-in limitation of our approach. However, the choice of having arbitrary values of α_i for each ring is not attractive, since it would make the protection of the dielectric rings a more difficult task and in addition it would not define a relatively smooth surface of zero potential, so that the abrupt variation of α_i would impart an undesired amount of temperature in the beam. The actual choice in practice is that of introducing a smooth function $\alpha(z)$. By employing a WKB-type approximation our method can be extended to take into account such a choice.

The purpose of this paper is to demonstrate the applicability of our approach to a nonperiodic system. [Which type of nonperiodicity accomplishes the ultimate good (i.e., maximization of the strength of the interaction in the TWT or its minimization in a gyrotron-beam tunnel) is a question beyond the scope of this paper.] For such a first application, the system is simplified in two ways. The first simplification is that the inner radii of the metal and dielectric rings are both equal to α, as is already shown in Fig. 1. In practice, the structures actually employed in gyrotron-beam tunnels have the inner diameter of the dielectric rings somewhat larger than that of the adjacent conductor, in order to protect the dielectric from any stray electrons. This offset is, however, much smaller than the other dimensions of relevance, and we expect (and verify *a posteriori*) that it can be safely ignored. For cases where such

an offset is of importance, this simplification can by removed by incorporating the appropriate boundary conditions in the expressions for field structure in the region $\rho > \alpha$. The second simplification refers to the boundary conditions at $z = 0$ and $z = L_0$, which in Section II are assumed periodic. As a consequence, the present implementation of our approach applies to systems containing many wavelengths along the axis, contrary to the *CASCADE* code, which also can handle, for example, dielectrics with a triangular cross section or very short cavities [17]. This simplification can also be removed by implementing the appropriate Sturm–Liouville boundary conditions.

The mathematical formulation of a simplified corrugated waveguide is presented in Section II. An infinite system of equations is derived, which is solved numerically by letting its finite-size determinant become equal to zero. This analysis is used in Section III, where a numerical code (*FISHBONE-TM*) is developed and its main steps are described. Examples for both a periodic and a nonperiodic corrugated waveguide are presented in Section IV, and the results (dispersion relation, field components, and quality factor) are compared with those obtained by the *CASCADE* code.

II. Mathematical Formulation

The cross-sectional geometry of the circular waveguide has already been described and is shown in Fig. 1. In such a structure, out of the variety of modes which can in principle propagate, we are currently interested in the development in the electron beam of the Langmuir mode, which can couple conveniently with the lowest frequency azimuthally symmetric TM mode. In order to demonstrate our approach in the simplest case, we confine our attention to systems where: 1) the electromagnetic field is independent of the φ coordinate, that is $\partial/\partial\varphi = 0$; and 2) only the fundamental TM mode is excited, that is $H_z(\rho, z) = 0$ everywhere. A time dependence of $\exp(+j\omega t)$ is assumed (and suppressed in the notation) throughout the analysis.

The analysis follows established procedures: First, the longitudinal component of the electric field $E_z(\rho, z)$ is considered in each region separately and, then, the other components of the electromagnetic field are expressed in terms of $E_z(\rho, z)$ employing Maxwell's equations. Then, the boundary conditions are forced on the interfaces that separate the various regions of the waveguide. The satisfaction of the boundary conditions gives rise to the homogeneous infinite set of equations that governs the problem.

To obtain an appropriate expansion for $E_z(\rho, z)$ in the empty inner cylinder ($\rho < \alpha$), we consider region V (the entire length L_0) as the unit cell of a periodic structure. Strictly speaking, the coupling of region V to its environment at $z = 0$ and at $z = L_0$, expressed by appropriate reflection and transmission coefficients, defines a Sturm–Liouville problem. However, the long length L_0 is expected to contain many wavelengths, so that the results are anticipated to be largely insensitive to the actual type of boundary conditions imposed at $z = 0$ and $z = L_0$. For simplicity, we choose periodic boundary conditions, thus Floquet's theorem allows for the propagating wave in the empty cylindrical region to be expanded as a sum of Bloch components [12]–[14]

$$E_z(\rho, z) = \sum_{n=-\infty}^{+\infty} A_n F_{0n}(\rho) \exp(-jk_n z), \quad \text{for} \quad 0 < \rho < \alpha \quad \text{and} \quad 0 < z < L_0 \tag{1}$$

each with axial wavenumber $k_n = k + n(2\pi/L_0)$, while A_n are unknown expansion coefficients to be determined. If the frequency ω is real, then depending on the value of n, the transverse variation is either oscillatory (with characteristic length h_n^{-1}) or evanescent (with characteristic length t_n^{-1}), where h_n and t_n are defined as $h_n^2 = (\omega/c)^2 - k_n^2$ and $t_n^2 = k_n^2 - (\omega/c)^2$, respectively. Of course, the same definition can be used also for complex ω. The function $F_{0n}(\rho)$ is given by the radial dependence of the transverse mode TM_{0n}

$$F_{0n}(\rho) = \begin{cases} J_0(h_n\rho), & \text{for} \mathrm{Re}(h_n^2) > 0, \mathrm{Re}(h_n) > 0, \mathrm{Im}(h_n) > 0 \\ I_0(t_n\rho), & \text{for} \mathrm{Re}(t_n^2) > 0, \mathrm{Re}(t_n) > 0, \mathrm{Im}(t_n) < 0. \end{cases} \tag{2}$$

In the latter equation, $J_0(x)$ and $I_0(x)$ are, respectively, the Bessel function and the modified Bessel function, both of the first kind. The corresponding functions of the second kind have been dropped, in order to keep the fields finite at $\rho = 0$.

Mathematically, it would suffice to use a single definition [e.g., $F_{0n}(\rho) = J_0(h_n\rho)$], since the frequency is expected to be complex due to the complex permittivity. However, since the loss tangent is relatively small, the frequency is expected to be almost real. Thus, we have opted to use the dual definition of F_{0n}, both in order to maintain a better feeling for the radial dependence and to facilitate a numerical implementation based on an expansion about the (large) real value of the argument.

Similarly, in each dielectric region $R_i(\alpha < \rho < D_i, z_i < z < z_i + b_i, i = 1, 2, \cdots, P)$ the longitudinal component of the electric field is represented by a Fourier series as an infinite sum of the corresponding standing eigenwaves

$$E_{zi}(\rho, z) = \sum_m B_{mi} G_{0mi}(\rho) \cos[\kappa_{mi}(z - z_i)], \quad \text{for} \quad \alpha < \rho < D_i \quad \text{and} \quad z_i < z < z_i + b_i. \tag{3}$$

In this equation no sine term is included, for the radial component of the electric field to vanish at $z = z_i$. Furthermore, the axial wavenumber κ_{mi} is equal to $m\pi/b_i$, in order for the radial component of the electric field to vanish at $z = z_i + b_i$. Therefore, the summation is to be performed over all nonnegative integers m. Finally, B_{mi} are unknown expansion coefficients to be determined, while the function $G_{0mi}(\rho)$ is a linear combination of $J_0(\rho)$ and $Y_0(\rho)$ or $I_0(\rho)$ and $K_0(\rho)$, where $Y_0(\rho)$ and $K_0(\rho)$ are, respectively, the Neumann function and the modified Bessel function of the second kind. Taking into account the boundary condition at $\rho = D_i$ (i.e., $E_{zi} = 0$) the function $G_{0mi}(\rho)$ is given by the equation

$$G_{0mi}(\rho) = \begin{cases} J_0(g_{mi}\rho)Y_0(g_{mi}D_i) - J_0(g_{mi}D_i)Y_0(g_{mi}\rho), \\ \mathrm{Re}(g_{mi}^2) > 0, \mathrm{Re}(g_{mi}) > 0, \mathrm{Im}(g_{mi}) > 0 \\ I_0(s_{mi}\rho)K_0(s_{mi}D_i) - I_0(s_{mi}D_i)K_0(s_{mi}\rho), \\ \mathrm{Re}(s_{mi}^2) > 0, \mathrm{Re}(s_{mi}) > 0, \mathrm{Im}(s_{mi}) < 0 \end{cases} \tag{4}$$

with $g_{mi}^2 = (\omega/c)^2\varepsilon_i - \kappa_{mi}^2$ and $s_{mi}^2 = \kappa_{mi}^2 - (\omega/c)^2\varepsilon_i$ representing the inverse of the transverse characteristic length inside each dielectric region, analogous to h_n and t_n in the empty region V. Although it is mathematically redundant, we have chosen to give the dual definition of G_{0mi} for the same reasons as for F_{0n}.

Finally, the electromagnetic field inside the perfect conductors (regions $C_i, i = 1,2,\cdots,P$ and outside the cylindrical waveguide) should be zero.

Then, taking into account that the electromagnetic field has no azimuthal dependence and that $H_z(\rho,z) = 0$ for the TM modes considered, the transverse field components in each region of the circular waveguide are immediately obtained from Maxwell's equations: The components $E_\rho(\rho,z)$ and $H_\varphi(\rho,z)$ are proportional to the radial derivative of $E_z(\rho,z)$, while $E_\varphi(\rho,z) = 0$ and $H_\rho(\rho,z) = 0$ everywhere.

The tangential electric-field component should be continuous at the interface $\rho = \alpha$. Taking into account the alternative presence of dielectric and conducting material, this condition gives

$$E_z(\alpha,z) = E_{zi}(\alpha,z) \quad \text{for} \quad z_i < z < z_i + b_i, \quad i = 1,2,\cdots,P \tag{5a}$$

$$E_z(\alpha,z) = 0 \quad \text{for} \quad z_i + b_i < z < z_i + L_i, \quad i = 1,2,\cdots,P \tag{5b}$$

or equivalently, using (1) and (3)

$$\sum_{q=-\infty}^{+\infty} A_q F_{0q}(\alpha)\exp(-jk_q z) = \left\{ \begin{array}{c} \displaystyle\sum_{m=0}^{+\infty} B_{mi} G_{0mi}(\alpha)\cos[\kappa_{mi}(z-z_i)] \\ \text{for} \quad z_i < z < z_i + b_i \\ 0 \quad \text{for} \quad z_i + b_i < z < z_i + L_i \end{array} \right\}. \tag{6}$$

Using orthogonality, (i.e., multiplying both sides of (6) by $\exp(+jk_n z)$ and integrating over the length of the waveguide), we obtain

$$A_n F_{0n}(\alpha) L_0 = \sum_{i=1}^{P} \exp(+jk_n z_i) \cdot \sum_{m=0}^{+\infty} B_{mi} G_{0mi}(\alpha) R(k_n, \kappa_{mi}, b_i) \tag{7}$$

where

$$R(k_n,\kappa_{mi},b_i) = \int_0^{b_i} \exp(+jk_n z)\cos(\kappa_{mi} z)\, dz = \left\{ \begin{array}{ll} jk_n \dfrac{1 - e^{jk_n b_i}(-1)^m}{k_n^2 - \kappa_{mi}^2}, & k_n \neq \pm\kappa_{mi} \\ \dfrac{b_i}{2}(1+\delta_{m0}), & k_n = \pm\kappa_{mi} \end{array} \right\} \tag{8}$$

and δ_{m0} is the Kronecker delta. Equation (7) holds for all integer values of n and represents an infinite set of equations, one for each value of n, that relates the expansion coefficients $A_n, n \in Z$, of the field in the empty inner region with the expansion coefficients $B_{mi} (i = 1,2,\cdots,P$ and $m = 0,1,2,\cdots)$ of the field inside the dielectric rings.

On the other hand, the tangential magnetic field should be continuous at the interface of the empty inner cylinder and the dielectric rings. This leads to the equation

$$H_\varphi(\alpha,z) = H_{\varphi i}(\alpha,z), \quad \text{for} \quad z_i < z < z_i + b_i; \quad i = 1,2,\cdots,P \tag{9}$$

or equivalently, using the expressions for the azimuthal magnetic field

$$\sum_{n=-\infty}^{+\infty} \frac{A_n}{h_n^2} F'_{0n}(\alpha)\exp(-jk_n z) = \sum_{m=0}^{+\infty} \frac{\varepsilon_i B_{mi}}{g_{mi}^2} G'_{0mi}(\alpha)\cos[\kappa_{mi}(z-z_i)], \quad \text{for} \quad z_i < z < z_i + b_i. \tag{10}$$

Multiplying (10) by $\cos[\kappa_{qi}(z - z_i)]$ and integrating over the length of each dielectric ring, one obtains

$$\frac{b_i \varepsilon_i B_{mi}}{2 g_{mi}^2} G'_{0mi}(\alpha)(1+\delta_{m0}) = \sum_{n=-\infty}^{+\infty} \frac{A_n}{h_n^2} F'_{0n}(\alpha)\exp(-jk_n z_i) R(-k_n, \kappa_{mi}, b_i). \tag{11}$$

The latter equation holds for $i = 1,2,\cdots,P$ and for all nonnegative integer values of m and represents a second infinite set of equations relating A_n to B_{mi} (for each i). The derivatives $F'_{0n}(\rho) = \partial F_{0n}/\partial\rho$ and $G'_{0mi}(\rho) = \partial G_{0mi}/\partial\rho$ arise out of the expressions for $H_\varphi(\rho,z)$. Equation (11) also satisfies the boundary conditions for εE_ρ at the interface $\rho = \alpha$.

Solving (11) for B_{mi} and substituting into (7), one obtains the linear system

$$\sum_{\ell=-\infty}^{+\infty} A_\ell X_{\ell,n} = A_n \Psi_n, \qquad n \in Z \tag{12}$$

where

$$X_{\ell,n} = \frac{F'_{0\ell}(\alpha)}{h_\ell^2} \sum_{i=1}^{P} \frac{e^{j(k_n - k_\ell)z_i}}{\varepsilon_i b_i} \cdot \sum_{m=0}^{+\infty} \frac{g_{mi}^2 G_{0mi}(\alpha)}{G'_{0mi}(\alpha)} \cdot \frac{1}{(1+\delta_{m0})} R(k_n,\kappa_{mi},b_i) R(-k_n,\kappa_{mi},b_i) \tag{13}$$

$$\Psi_n = \frac{1}{2} L_0 F_{0n}(\alpha). \tag{14}$$

The eigenvalue problem of (12), with the associated definition of $X_{\ell,n}$ and Ψ_n, concludes the formalism of the analysis: Setting the complex determinant equal to zero gives, e.g., for any given value of k the frequency ω, while the field components are subsequently obtained from the relevant equations. For numerical computations, one can truncate the infinite summations in (12) and (13) to $l = \pm N_{\max}$ and $m = M_{\max}$, respectively. This results to a system of $(2N_{\max} + 1)$ equations.

For cases of practical interest, the permittivity ε_i of the dielectric rings is either real (e.g., in a TWT, where losses are undesired), or complex, but with relatively not too large loss-tangent (e.g., in the gyrotron-beam tunnel, where the vacuum requirements represent a serious limitation on the choice for the material). In addition, since the application of this analysis to the gyrotron-beam tunnel aims at suppressing any interaction, high accuracy in the value of the frequency is not a critical requirement. For these reasons, we can neglect the imaginary part of ε_i, solve the eigenvalue problem with real arithmetic to obtain the real value of ω and the spatial dependence of the fields, and finally use the imaginary part of ε_i to obtain the quality factor Q of the system.

For the quality factor, the definition based on energy is employed, for example:

$$\frac{\omega}{Q} W_{em} = P_{\text{loss}} \tag{15}$$

where the stored electromagnetic energy is the integral of $\frac{1}{4}[\varepsilon_0|\vec{E}|^2 + \mu_0|\vec{H}|^2]$ over the total volume of the system, while the power loss is the summation of the dissipated power P_{diss} in the dielectric rings due to their complex dielectric permittivity and the refraction losses P_{refr}. The former is obtained as the integral of $\frac{1}{2}\vec{J}_{\text{con}} \cdot \vec{E}^*$ in the dielectric volume, with the introduction of the ohmic current density $\vec{J}_{\text{con}} = \sigma\vec{E} = j\omega \text{Im}[\varepsilon_i]\vec{E}$, while the latter is given by the integral of $\frac{1}{2}\,\text{Re}[\vec{E} \times \vec{H}^*] \cdot \hat{z}$ over the cross section of the inner region. Once Q is calculated, the conversation of electromagnetic energy allows for the imaginary part of ω to be obtained from $\text{Im}[\omega] = \text{Re}[\omega]/2Q$.

III. Numerical Implementation

The analysis developed in the previous section has been implemented in the numerical code *FISHBONE-TM*. The structure of this code is as follows.

a) The input parameters (dimensional or dimensionless) are requested in an interactive format.

b) To facilitate the convergence, as the initial estimates for ω, the cutoff frequencies are used for a waveguide of infinite length, loaded with a dielectric of permittivity ε_i and width $D_i - \alpha, i = 1, 2, \cdots, P$. In this step, the bisection method is used to estimate the cutoff frequency ω.

c) The values of $N_{\max}$ and $M_{\max}$, needed to truncate the summations in (12) and (13), are interactively chosen.

d) The eigenvalue problem of (12) is solved for either one value or for a range of values of the wavenumber k, as specified, using as an initial estimate the cutoff frequency ω of step b). At first, the (conservative) bisection method is used with small values for $N_{\max}$ and $M_{\max}$ (namely 3 and 1, respectively) to yield the first approximation of the root ω. Subsequently, the code has the possibility of interactively increasing the values of $N_{\max}$ and $M_{\max}$ and the extremely fast secant method is applied to improve on the accuracy without running the danger of defocusing from the root.

e) For every pair (ω, k) the electromagnetic field components are calculated in each region and their continuity at the interface is checked. For satisfactory continuity of the fields at the interfaces, the values of $N_{\max}$ and $M_{\max}$ have to be taken greater than 20 and 10, respectively.

f) The numerical code thus provides as output the dispersion relation $\omega(k)$ [by repeating step d)] and for every pair (ω, k) the fields at any position, the energy harmonics and the quality factor of the corrugated waveguide.

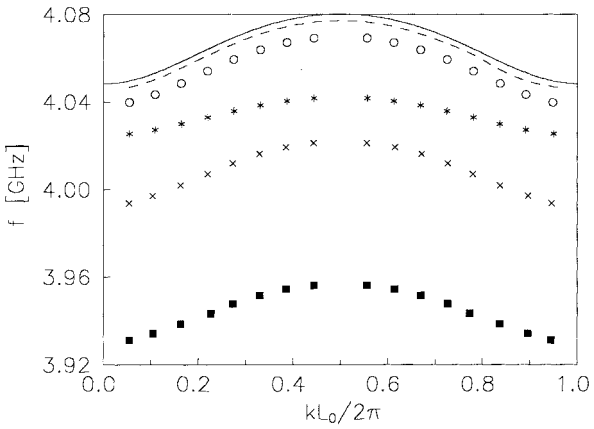

Fig. 2. The dispersion relation $\omega(k)$ for the first TM mode in the simplified periodic geometry without losses, as obtained by the *FISHBONE-TM* code (solid line) and by the *CASCADE* one (dashed line). In addition, results from the *CASCADE* code are shown for the exact periodic geometry without losses (asterisks), as well as for the simplified periodic geometry with $\varepsilon = 7 + j0.5$ (empty circles), $\varepsilon = 7 + j1.4$ (crosses), and $\varepsilon = 7 + j2.1$ (full squares).

To test the convergence of the numerical procedure and the accuracy of the results, the code *FISHBONE-TM* has been run in parallel with the code *CASCADE* using the CRAY Y-MP/M94 of Ecole Polytechnique Federale de Lausanne (EPFL). The latter code gives the frequency and the field distribution and a subsequent Fourier analysis of the dependence $E_z(z)$ gives the dispersion relation.

IV. Numerical Convergence, Results, and Discussion

In order to establish the convergence properties in what follows, numerical computations are presented for one periodic and one nonperiodic geometry. The parameters of each are given in Table I. All fields are normalized in terms of $E_0 = E_z(\rho = 0, z = 0)$, i.e., the value of the total (including all Bloch Harmonics) axial electric field on the axis.

A. Periodic Structure

In this case, the structure is assumed to consist of a large number of identical segments, with the characteristics given in the first row of Table I. For this geometry, excellent convergence (accurate with 1 out of 4000) of the dispersion relation $\omega(k)$ for the first TM mode is obtained by taking $N_{\max} = 2$ and $M_{\max} = 1$. The results are shown by the solid curve in Fig. 2. It is noted that the frequency is indeed close to the first cutoff frequency of an infinite waveguide having an inner radius of 6 mm cladded by a dielectric ring of radius 8 mm (with the real part of its permittivity equal to seven). Running the *CASCADE* code for the same simplified geometry and with no losses in the dielectric rings the dashed line of

TABLE I
SAMPLE GEOMETRIES

a [mm]	D_i [mm]	ε_i	b_i [mm]	L_i [mm]
A. Periodic Structure				
6	14	7.0+j0.5	3	6
B. Non–Periodic Structure				
6	14	8.0 + j0.4	1	4
6	16	7.5 + j0.6	4	6
6	18	10 + j0.1	2	4
6	20	9.0 + j0.8	7	10

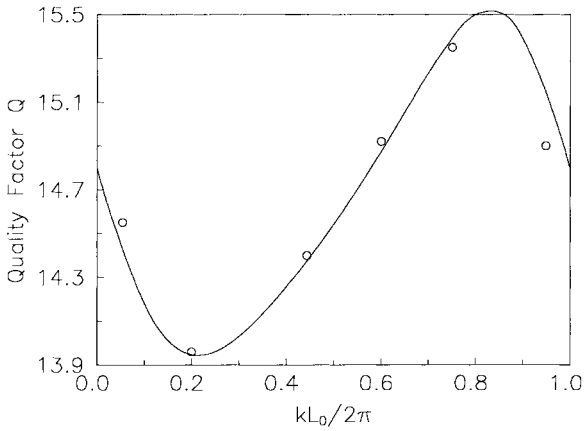

Fig. 3. The quality factor $Q(k)$ for the first TM mode for the simplified periodic structure, obtained by the *FISHBONE-TM* code (solid line) and by the *CASCADE* code (empty circles).

Fig. 2 has been produced. It can be seen that the frequency difference is indeed negligible.

As has been mentioned in the introduction, the realistic system employs a somewhat different inner radius for the dielectric and conducting rings, while our analysis (and consequently our numerical code) employs a somewhat simplified model, which assumes an identical radius α. To assess the effects caused by this discrepancy, the *CASCADE* code has also been run with a radius offset of 1 mm (exact geometry) and no losses in the dielectric rings. The results are also presented by asterisks in Fig. 2. It can be seen that the exact geometry gives a frequency of about 40 MHz lower than in our approximation. Clearly, this discrepancy of less than 1% is, in general, of no significance unless a very accurate design is required.

An additional simplification in the *FISHBONE-TM* code lies in the assumption of no losses in the dielectric rings. To assess this simplification the *CASCADE* code has been run with $\varepsilon = 7 + j0.5$ (empty circles), $\varepsilon = 7 + j1.4$ (crosses), and $\varepsilon = 7 + j2.1$ (full squares). It can be seen that the *FISHBONE-TM* code slightly overestimates the frequency. However, even with a loss tangent as high as $2.1/7 = 0.3$, the discrepancy is less than 3%.

Satisfactory convergence of the quality factor curve $Q(k)$ with respect to $N_{\max}$ and $M_{\max}$ is obtained for the small values three and one, respectively. From Fig. 3, it is evident that both codes give almost identical results for the quality factor.

In Fig. 4(a) and (b), the number of modes and the central processing unit (CPU) time (in seconds) versus the frequency error (in kHz) are plotted for both codes. It can be seen that a frequency error less than 100 kHz is achieved by using nine modes in the *FISHBONE-TM* code and 32 modes in the *CASCADE* one, while the required CPU time is 10 and 15 s, respectively. [These comparisons are based on an earlier version of the *FISHBONE-TM* code, in which the bisection method was used for all frequency calculations. With the additional implementation of the secant method in step d), the current (final) version of the *FISHBONE-TM* code has been seen to be about 50% faster than the earlier version.]

To verify the equivalence of the two codes, the variation of the normalized longitudinal electric-field component $E_z(\rho)/E_0$ with respect to the radius ρ at the axial position $z = 0.3b_1$ (dielectric region) and at lower cutoff ($kL_0/2\pi = 0.01$) is presented in Fig. 5(a). In particular, in this figure the results obtained by the *FISHBONE-TM* code for the simplified geometry and those obtained by the *CASCADE* for the simplified and the exact one are presented. It is obvious that both codes give almost identical results for the simplified geometry, while the results for the simplified and the exact geometry have a slight difference. Furthermore, in Fig. 5(b), the variation of the normalized longitudinal electric-field component $E_z(\rho)/E_0$ with respect to the radius ρ at the axial position $z = b_1 + 0.3(L_1 - b_1)$ (copper region) and at lower cutoff ($kL_0/2\pi = 0.01$) is presented for the simplified geometry without losses. From this figure, it is evident that both codes give identical results. Finally, in Fig. 5(c), the results referred to the longitudinal variation of the normalized longitudinal electric-field component $E_z(z)/E_0$ at the interface ($\rho = \alpha$) and at lower cutoff ($kL_0/2\pi = 0.01$)

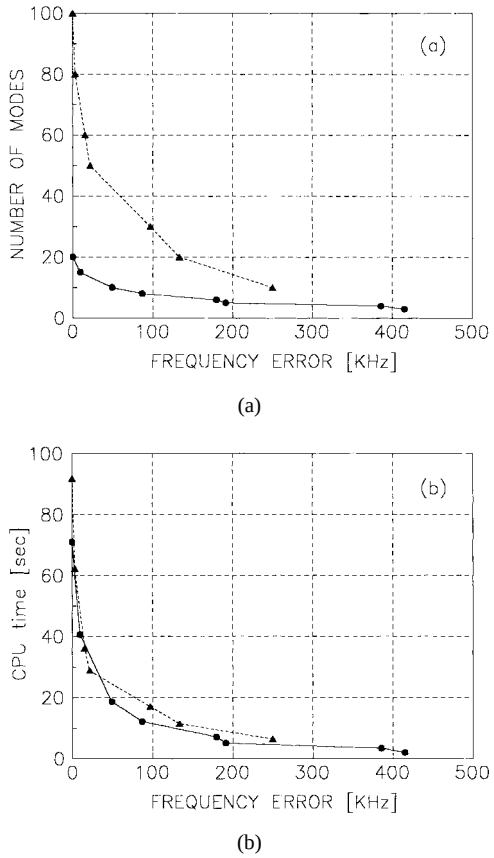

Fig. 4. (a) The required number of modes and (b) the CPU time (in s) needed for a given frequency error (in kHz) for the simplified periodic structure, obtained by the *FISHBONE-TM* code (solid line with full circles) and by the *CASCADE* code (dashed line with full triangles).

are presented for both the *FISHBONE-TM* and the *CASCADE* code for the simplified geometry. Clearly, both codes are also in very good agreement.

B. Nonperiodic Structure

As a reference nonperiodic structure, we have used the parameters in Table I. It has been seen that the number of modes required to obtain convergence in the dispersion relation curve $\omega(k)$ is now only slightly larger ($N_{\max} = 3$ and $M_{\max} = 3$). In Fig. 6, the dispersion relations obtained by the *FISHBONE-TM* and the *CASCADE* code for the simplified nonperiodic geometry are presented. From this figure, it is obvious that both codes are giving identical results, since the difference of 1.08 MHz (0.05%) is in practice negligible.

In Figs. 7 and 8 we present the variation of the normalized longitudinal electric-field component $E_z(\rho)/E_0$ with respect to the radius ρ at lower cutoff ($kL_0/2\pi = 0.01$) and at four axial positions z and facing the dielectric and metal rings, respectively. In these figures, the data from both codes are practically identical. As expected, in the case of nonperiodic geometry, the field components require for convergence higher values $N_{\max} = 50$ and $M_{\max} = 12$. Finally, in Fig. 9, the results are presented for the variation with z of the normalized longitudinal electric-field component $E_z(z)/E_0$ at the interface ($\rho = \alpha$) and at lower cutoff ($kL_0/2\pi = 0.01$). It is also clear that as expected the electric field becomes

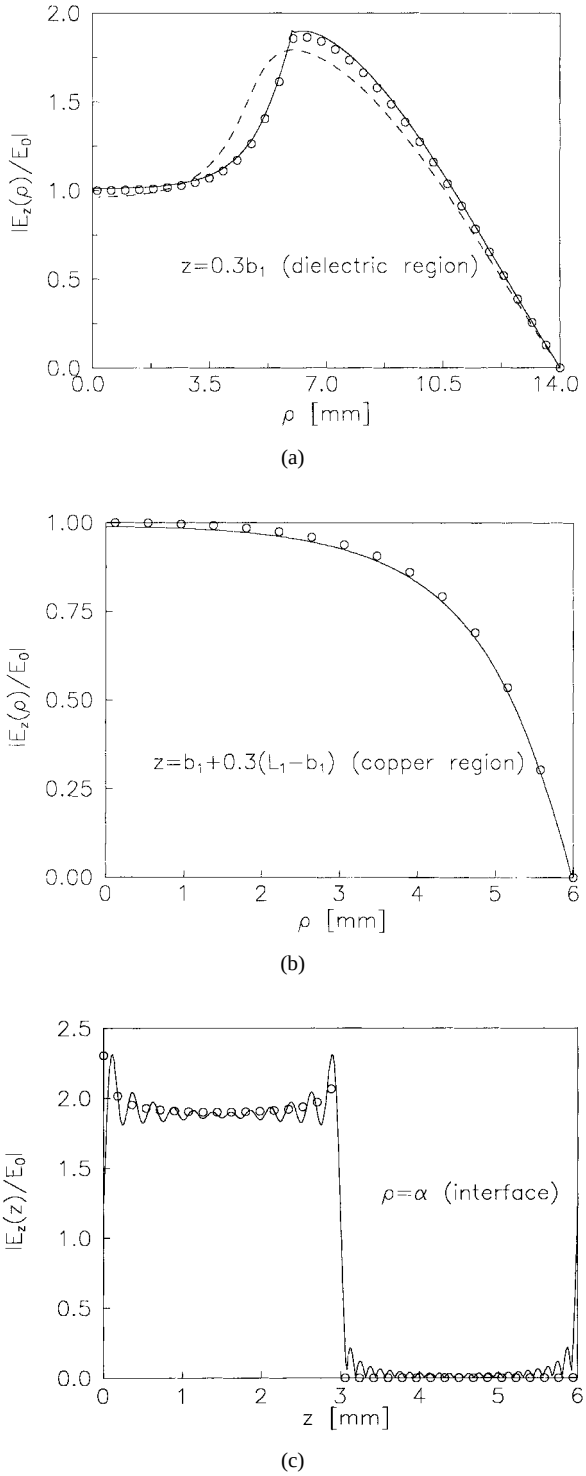

Fig. 5. (a) The variation of the normalized longitudinal electric field $E_z(\rho)/E_0$ with the radius ρ (in mm) at the axial position $z = 0.3b_1$ (dielectric region) and at lower cutoff ($kL_0/2\pi = 0.01$) for the periodic structure, obtained by the *FISHBONE-TM* code for the simplified geometry (solid line) by the *CASCADE* code for the simplified geometry (empty circles) and for the corresponding exact geometry without losses (dashed line). (b) The variation of the normalized longitudinal electric field $E_z(\rho)/E_0$ with the radius ρ (in mm) at the axial position $z = b_1 + 0.3(L_1 - b_1)$ (copper region) and at lower cutoff ($kL_0/2\pi = 0.01$) for the simplified periodic structure without losses, obtained by the *FISHBONE-TM* code (solid line) and by the *CASCADE* code (empty circles). (c) The variation of the normalized longitudinal electric field $E_z(z)/E_0$ with the axial position z (in mm) at the interface ($\rho = \alpha$) and at lower cutoff ($kL_0/2\pi = 0.01$) for the simplified periodic structure, obtained by the *FISHBONE-TM* code (solid line) and by the *CASCADE* code (empty circles).

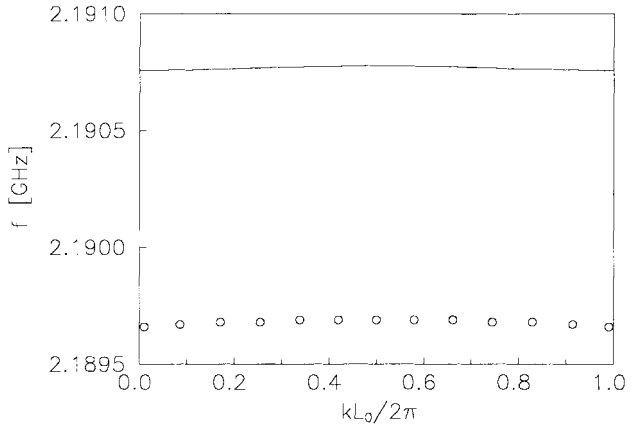

Fig. 6. The dispersion relation $\omega(k)$ for the first TM mode for the simplified nonperiodic structure obtained by the *FISHBONE-TM* code (solid line) and by the *CASCADE* code (empty circles).

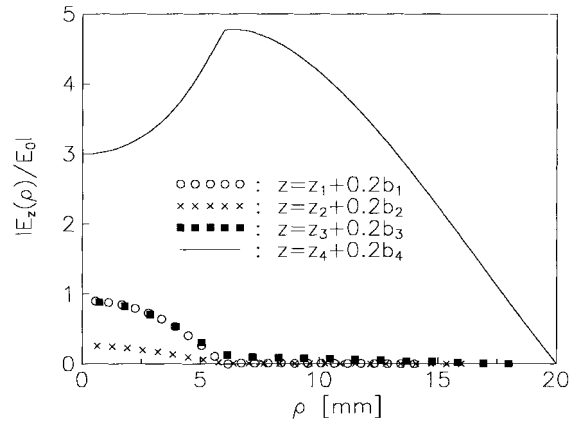

Fig. 7. The variation of the normalized longitudinal electric field $E_z(\rho)/E_0$ with the radius ρ (in mm) for the simplified nonperiodic structure at lower cutoff $(kL_0/2\pi = 0.01)$ at axial positions $z = z_1 + 0.2b_1$ (first dielectric region, empty circles), $z = z_2 + 0.2b_2$ (second dielectric region, crosses), $z = z_3 + 0.2b_3$ (third dielectric region, full squares), and $z = z_4 + 0.2b_4$ (forth dielectric region, solid line).

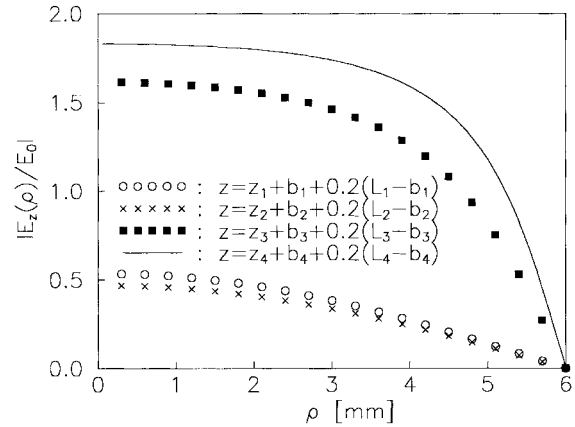

Fig. 8. The variation of the normalized longitudinal electric field $E_z(\rho)/E_0$ with the radius ρ (in mm) for the simplified nonperiodic structure at lower cutoff $(kL_0/2\pi = 0.01)$ and at axial positions $z = z_1 + b_1 + 0.2(L_1 - b_1)$ (first copper region, empty circles), $z = z_2 + b_2 + 0.2(L_2 - b_2)$ (second copper region, crosses), $z = z_3 + b_3 + 0.2(L_3 - b_3)$ (third copper region, full squares), and $z = z_4 + b_4 + 0.2(L_4 - b_4)$ (forth copper region, solid line).

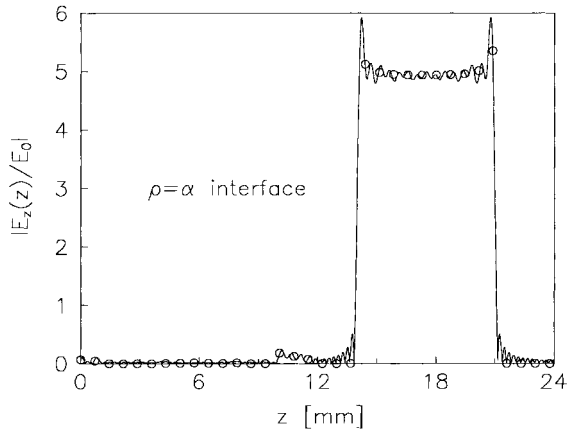

Fig. 9. The variation of the normalized longitudinal electric field $E_z(z)/E_0$ with the axial position z (in mm) at the interface $(\rho = \alpha)$ and at lower cutoff $(kL_0/2\pi = 0.01)$ for the simplified nonperiodic structure, obtained by the *FISHBONE-TM* code (solid line) and by the *CASCADE* code (empty circles).

significant in the region of the forth dielectric ring, since the operating frequency is close to the cutoff frequency of its corresponding dielectric loaded infinite waveguide.

V. Conclusion

In this paper, the dispersion characteristics of a waveguide with nonperiodic dielectrically loaded corrugations have been investigated for the azimuthally symmetric TM waves. Techniques developed for a periodic system have been extended to describe the nonperiodic structure and the results obtained by this method (*FISHBONE-TM* code) have been found to be in very good agreement with those obtained by an established code (*CASCADE*). The main advantage of this code compared to the *CASCADE* one is that it gives the dispersion relation directly and with only a small number of modes, resulting in respectable savings on CPU time. Furthermore, in cases when the imaginary part of permittivity is not too large, neglecting this part has been seen not to affect the dispersion relation. The results obtained indicate the possibility of extending this method to more complicated cases, such as modes with no azimuthal symmetry.

Acknowledgment

Fruitful discussions with Prof. M. Q. Tran of CRPP as well as the constructive comments of the reviewers are kindly acknowledged.

References

[1] W. Lawson, J. P. Calame, B. P. Hogan, M. Skopec, C. D. Striffler, and V. L. Granatstein, "Performance characteristic of a high-power x-band two-cavity gyroklystron," *IEEE Trans. Plasma Sci.*, vol. 20, pp. 216–223, 1992.

[2] I. I. Antakov, I. G. Gachev, and E. V. Zasypkin, "Self-excitation of spurious oscillations in the drift region of gyrotron and their influence on gyrotron operation," *IEEE Trans. Plasma Sci.*, vol. 22, pp. 878–882, 1994.

[3] M. Pedrozzi, S. Alberti, and M. Q. Tran, "Parasitic mode excitation in gyrotron-beam tunnels," in *Proc. 20th Int. Conf. Infrared and Millimeter Waves*, Lake Buena Vista, FL, 1995, pp. 134–135.

[4] L. Schachter and J. A. Nation, "Analytical method for studying a quasiperiodic disk loaded waveguide," *Appl. Phys. Lett.*, vol. 63, no. 17, pp. 2441–2443, 1993.

[5] G. L. James, "Analysis and design of TE_{11}-to-HE_{11} corrugated cylindrical waveguide mode converters," *IEEE Trans. Microwave Theory Tech.*, vol. MTT-29, pp. 1059–1066, 1981.
[6] A. Rekiouak, B. R. Cheo, G. Wurthman, and C. Bates, "A slow-wave structure for gyro-TWA H_{11} operation," *IEEE Trans. Microwave Theory Tech.*, vol. 42, pp. 1091–1094, 1994.
[7] M. Celuch-Marcysiak and W. K. Gwarek, "Spatially looped algorithms for time-domain analysis of periodic structures," *IEEE Trans. Microwave Theory Tech.*, vol. 43, pp. 860–865, 1995.
[8] H. Guo, Y. Carmel, W. R. Lou, L. Chen, J. Rodgers, D. K. Abe, A. Bromborsky, W. W. Destler, and V. L. Granatstein, "A novel highly accurate synthetic technique for determination of the dispersive characteristics in periodic slow wave circuits," *IEEE Trans. Microwave Theory Tech.*, vol. 40, pp. 2086–2094, 1992.
[9] Y. Carmel, H. Guo, W. R. Lou, D. K. Abe, A. Bromborsky, V. L. Granatstein, and W. W. Destler, "Novel method for determining the electromagnetic dispersion relation of periodic slow-wave structures," *Appl. Phys. Lett.*, vol. 57, no. 13, pp. 1304–1306, 1992.
[10] Md. R. Amin, K. Ogura, H. Kitamura, K. Minami, T. Watanabe, Y. Carmel, W. Main, J. Weaver, W. W. Destler, and V. L. Granatstein, "Analysis of the electromagnetic waves in an overmoded finite length slow-wave structure," *IEEE Trans. Microwave Theory Tech.*, vol. 43, pp. 815–822, 1995.
[11] V. Rizzoli and A. Lipparini, "Bloch-wave analysis of stripline and microstrip array slwo-wave structures," *IEEE Trans. Microwave Theory Tech.*, vol. MTT-29, pp. 143–150, 1981.
[12] A. F. Harvey, "Periodic and guiding structures at microwave frequencies," *IRE Trans. Microwave Theory Tech.*, vol. MTT-8, pp. 30–61, 1960.
[13] C. Elachi, "Waves in active and passive periodic structures: A review," *Proc. IEEE*, vol. 64, pp. 1666–1698, 1976.
[14] R. E. Collin, *Foundations For Microwave Engineering*, 2nd ed. New York: McGraw-Hill, 1992, ch. 8.
[15] J. M. Neilson, P. E. Latham, M. Caplan, and W. G. Lawson, "Determination of the resonant frequencies in a complex cavity using the scattering-matrix formulation," *IEEE Trans. Microwave Theory Tech.*, vol. 37, pp. 1165–1170, 1989.
[16] W. G. Lawson and P. E. Latham, "The scattering-matrix formulation for overmoded coaxial cavities," *IEEE Trans. Microwave Theory Tech.*, vol. 40, pp. 1973–1977, 1992.
[17] G. P. Saraph, W. Lawson, P. E. Latham, J. Cheng, M. Castle, J. P. Calame, G. S. Nusinovich, M. Reiser, and V. L. Granatstein, "Designs of two and three cavity gyroklystron amplifiers operating at fundamental, second, and fourth harmonics," in *Proc. 20th Int. Conf. Infrared and Millimeter Waves*, Lake Buena Vista, FL, 1995, pp. 421–422.

Ioannis G. Tigelis (M'92) was born in Lamia, Greece, in 1964. He received the Diploma of Electrical Engineering and the Dr.Eng. degrees from the National Technical University of Athens (NTUA), Athens, Greece, in 1986 and 1990, respectively.

In April 1991, he was elected Lecturer at the Physics Department, University of Athens, Athens, Greece. His research interests include microwave theory and applications as well as fiber optics telecommunications.

Marco Pedrozzi was born in Lugano, Switzerland, in 1964. He received the Dipl.-Ing. Degree in physics from the Swiss Federal Institute of Technology Lausanne, Switzerland, in 1990, and the Dr. ès Sciences degree from Ecole Polytechnique Federale de Lausanne (EPFL), Lausanne, Switzerland, in 1997.

Beginning in 1990 he has served as Assistant in the Centre de Recherches en Physique des Plasmas (CRPP), Lausanne, Switzerland, where he works on quasioptical gyrotron development, microwave techniques, and charged beam instabilities.

Panayotis G. Cottis was born in Thessaloniki, Greece, in 1956. He received the Diploma in Mechanical and Electrical Engineering degree and the Dr.Eng. degree from the National Technical University of Athens (NTUA), Athens, Greece, in 1979, and 1984, respectively, and the M.Sc. degree from the University of Manchester (UMIST), Manchester, U.K., in 1980

In April 1985, he joined the Department of Electrical and Computer Engineering, National Technical University of Athens (NTUA), Athens, Greece, where he is currently a Professor. Since 1988 he has been serving as a Special Scientist at the Naval Academy of Greece. His research interests include microwave theory and applications, wave propagation in anisotropic media, electromagnetic scattering, and fiber optics.

John L. Vomvoridis was born in Thessaloniki, Greece, in 1947. He received the Diploma in Mechanical and Electrical Engineering degree from the National Technical University of Athens (NTUA), Athens, Greece, in 1970 and the Ph.D. from Northwestern University, Evanston, IL, in 1977.

After having worked at Northwestern University, the Naval Research Laboratory, Western Research Corporation and the Ministry of Research and Technology, he joined the faculty of the Department of Electrical and Computer Engineering, National Technical University of Athens, (NTUA), Athens, Greece, in 1984, where he is currently a Professor. His research interests include plasma physics, physics of charged particle beams, high-power microwave generation, and electrodynamics.